Journal of the Physical Society of Japan
Vol. 53, No. 2, February, 1984, pp. 811–818

# Dispersive Raman Mode of Layered Compound 2H–$MoS_2$ under the Resonant Condition

Tomoyuki SEKINE, Kunimitsu UCHINOKURA,
Tsuneo NAKASHIZU, Etsuyuki MATSUURA
and Ryozo YOSHIZAKI†

*Institute of Physics, University of Tsukuba,*
*Sakura-mura, Ibaraki 305*
†*Institute of Applied Physics, University of Tsukuba,*
*Sakura-mura, Ibaraki 305*

(Received April 11, 1983)

A frequency shift of a Raman peak is observed in 2H–$MoS_2$, when the exciting laser frequency $\omega_i$ is tuned across the A and B excitonic levels. The frequency shift decreases as $\omega_i$ increases. It can be explained as due to a resonant two-phonon Raman process of the successive emission of a dispersive longitudinal quasi-acoustic phonon and a dispersionless $E^2_{1u}$ phonon both along the $c$ axis. The translational exciton masses along the $c$ axis are estimated to be $(1.3\pm0.2)m_0$ for the $1s$ state of the A exciton and $(1.6\pm0.3)m_0$ for the $1s$ state of the B exciton. The observed Raman cross section is consistent with qualitative estimation in terms of this Raman process.

## §1. Introduction

Many investigations have been done in layered materials in view of the physical interest in two-dimensional properties. 2H–$MoS_2$ is one of the most familiar materials among the layered compounds and it has A and B excitonic sharp peaks in the absorption spectrum. Many studies of these excitons, however, have been restricted to the properties associated with their internal motions.[1,2]

The resonant Brillouin/Raman scattering has recently been understood to be an important method for obtaining precise information about the translational motions of the excitons in semiconductors. The resonant Brillouin scattering of excitonic polaritons by longitudinal and transverse acoustic (LA and TA) phonons has been reported on GaAs,[3,4] CdS,[5,6] CdTe,[7] CdSe,[8] ZnSe,[9] $HgI_2$,[10] 2H–$PbI_2$[11] and CuBr.[12] In the resonant Raman scattering (RRS) of CdS, Koteles and Winterling[13] have observed dispersive Raman peaks near a longitudinal optical (LO) phonon peak. The dispersive Raman peaks have been interpreted as two- or three-phonon process in which a polariton is scattered by emitting one or two acoustic phonons and then scattered by emitting an LO phonon. Oka and Cardona[14] have observed not only the scattering process of the acoustic-phonon emission followed by the LO-phonon emission but also that of the reversed order in the RRS of ZnTe. On the other hand, Yu and Shen[15] have observed three dispersive Raman peaks at the high-frequency side of a two-phonon Raman peak for the case where the incident laser frequency $\omega_i$ is above the $1s$ yellow excitonic level in $Cu_2O$ and they have assigned these peaks to three- and four-phonon Raman processes consisting of two optical phonons plus LA, 2LA and TA phonons. In their experiment there exists no polariton effect, because the exciton is dipole-forbidden.

The acoustic phonons, whose frequencies depend linearly on the wave vector $\boldsymbol{q}$, have played an important role in the dispersive Raman scattering. In principle, however, we can observe dispersive peaks involving dispersive phonons other than acoustic phonons in the RRS.

This is the first report on the translational motion of the excitons in 2H–$MoS_2$ and a dispersive Raman peak in which a dispersive optical phonons, i.e., a quasi-acoustic phonon, plays an important role. This Raman process is

characteristic of the layered structure. Moreover we discuss the Raman cross section of this peak.

## §2. Experimental Procedures

The RRS measurement has been performed using 450–800 nm laser lines at about 7 K. We obtain these laser lines by operating an argon (Spectra Physics 171–18) and a krypton (Spectra Physics 171–01) ion lasers and a dye laser (Spectra Physics 375) excited by these ion lasers. A typical linewidth of the dye-laser line is about 0.1 Å at 590 nm. A conventional backscattering geometry has been taken on cleaved surfaces of natural crystals. Raman spectra have been detected by a multichannel detector (IDARSS) of Tracor Northern through a Spex 1401 double monochromator. This multichannel detector has an array of 1024 photodiode detector elements in 25 mm × 2.5 mm area. In our experiments we have used an area of about 15 mm × 2.5 mm by masking the periphery, and this optical configuration covers the spectral range of about 150 $cm^{-1}$ at 17000 $cm^{-1}$. This detector is very useful for the RRS measurement because the whole spectrum is obtained simultaneously in a short exposure time. The obtained spectra have been corrected for the instrumental response.

## §3. Experimental Results and Discussion

The Raman spectra of 2H–$MoS_2$ were investigated mainly in the vicinity of the Raman-active $E^1_{2g}$ phonon at 386.5 $cm^{-1}$ and $A_{1g}$ phonon at 411.0 $cm^{-1}$. The RRS of these phonons has been reported previously by us.[16] Figure 1(a) shows Raman spectra when the incident laser frequency $\omega_i$ is tuned across the 1*s* state of the A exciton at 1.9449 eV and Fig. 1(b) shows Raman spectra if $\omega_i$ is above the 1*s* state of the B exciton at 2.1376 eV. These exciton energies were determined by the absorption measurement on the same sample at about 7 K. Under the resonant condition,

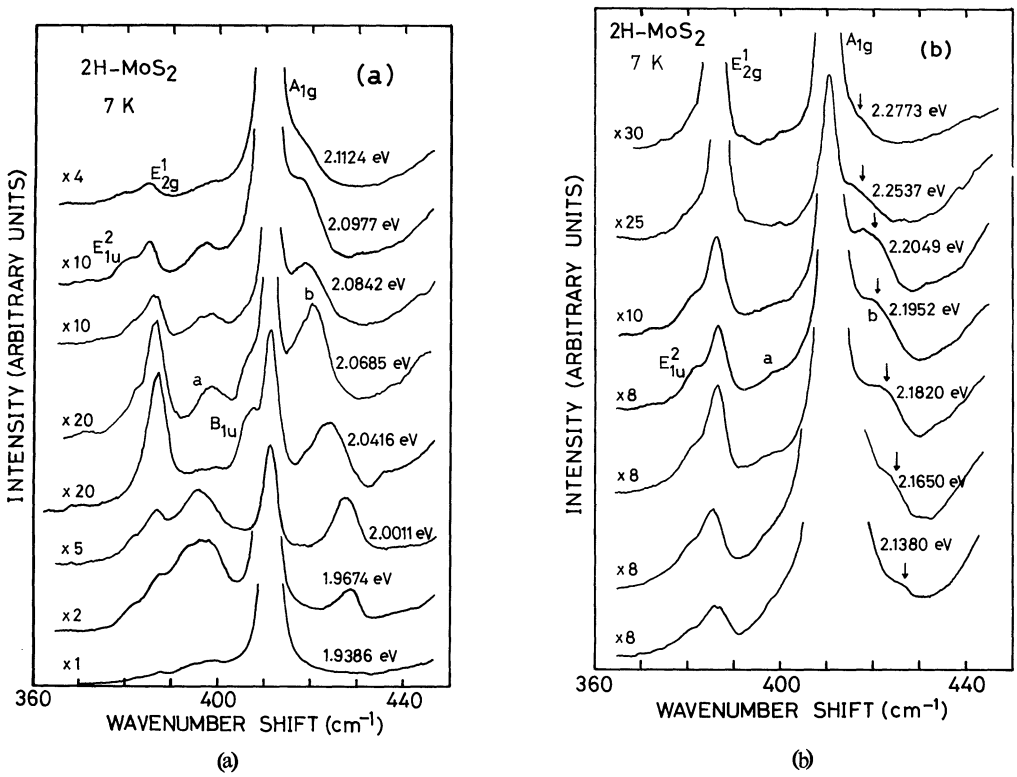


Fig. 1. Raman spectra of 2H–$MoS_2$ between 365 and 445 $cm^{-1}$ for various incident photon energies. Raman intensities are corrected for the instrumental response, but not for the absorption and reflection. (a) The incident photon energies are near the 1*s* level of the A exciton and below the 1*s* level of the B exciton. (b) The incident photon energies are above the 1*s* level of the B exciton.

many peaks were observed in the Raman spectra. At low-frequency sides of the $E^1_{2g}$ and $A_{1g}$ phonon peaks, Raman-inactive $E^2_{1u}$ and $B_{1u}$ phonons were observed because of the resonant effect. The small frequency splittings of the Davydov pairs (($E^2_{1u}$, $E^1_{2g}$) and ($B_{1u}$, $A_{1g}$)) reflect the fact that the interlayer interaction is very weak and therefore the dispersion curves are flat along the $c$ axis.[17] The RRS of the $E^2_{1u}$ and $B_{1u}$ phonons will be reported in a separate paper.

If $\omega_i$ is just above the 1$s$ level of the A exciton, "b" peak appears at 429 $cm^{-1}$ as shown in Fig. 1(a) and it shifts to the lower frequency and approaches the $A_{1g}$ phonon line as $\omega_i$ increases. If $\omega_i$ crosses the 1$s$ level of the B exciton, it appears again at about 427 $cm^{-1}$ and the similar frequency shift is observed in Fig. 1(b). Figure 2 shows the frequencies of Raman peaks of 2H–$MoS_2$ between 365 and 445 $cm^{-1}$ as functions of $\omega_i$.

If we assume that the b peak comes from the two-phonon difference combination process in which an optical phonon is created and an acoustic phonon is annihilated, we should also observe the corresponding two-phonon sum combination process. But we have not observed the latter process. Furthermore there exists no optical phonon of the former process.[17] We can therefore attribute the observed dispersive peak b to a sum combination process. The frequency dependence of the b peak on $\omega_i$ is opposite to the frequency dependences observed in the RRS of the two-phonon process of excitonic polaritons by LO and acoustic phonons in CdS[13] and ZnTe[14] and in the RRS of the three- and four-phonon processes of $Cu_2O$[15] involving optical and acoustic phonons. In CdS, ZnTe and $Cu_2O$, acoustic phonons whose frequencies depend linearly on the wave vector $\boldsymbol{q}$ play an important role. The present result of the frequency shift of the dispersive Raman peak cannot be explained by the dispersion of the acoustic phonons. We must consider an optical phonon whose frequency decreases as $|\boldsymbol{q}|$ increases. Quasi-acoustic phonon along the $c$ axis has such a dispersion.[18] It is probable that mainly the polariton along the c direction forms an intermediate state in this Raman process, because the dispersion of the polariton along the c direction is much flatter than that in the $a$-$b$ plane and the group velocity can be expected to be small along the c direction.[3]

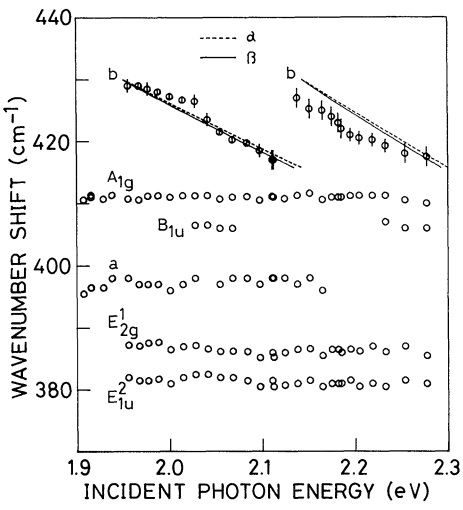


Fig. 2. The frequencies of all the observed Raman peaks of 2H–$MoS_2$ between 365 and 445 $cm^{-1}$ as functions of the incident photon energy. The dotted and solid curves represent the theoretical curves of the $\alpha$ and $\beta$ processes shown in Fig. 3, respectively.

As will be discussed later, an alternative explanation by an exciton picture may also be feasible. Our main purpose of the present paper is to report the observation of the dispersive Raman mode where the quasi-acoustic phonon plays an essential role, and the conclusion is not affected even if we use the exciton picture. Then we will apply the polariton picture to the present phenomenon tentatively, because polaritons are created inside the crystal having a dipole-allowed exciton and this picture simplifies our discussion.

We interpret the dispersive Raman peak as a two-phonon scattering process in which a polariton on the inner branch created in the crystal by an incident photon is scattered to the outer branch by emitting a quasi-acoustic phonon with a large wave vector parallel to the $c$ axis ($\Delta$ direction in the Brillouin zone), and then it is scattered by emitting an optical phonon into a photon-like-polariton final state, as shown in Fig. 3. To explain the magnitude of the frequency of this dispersive Raman peak, the participating phonons must be assigned as a longitudinal quasi-acoustic phonon ($\Delta_2$) and an $E^2_{1u}$ phonon ($\Delta_6$).* The

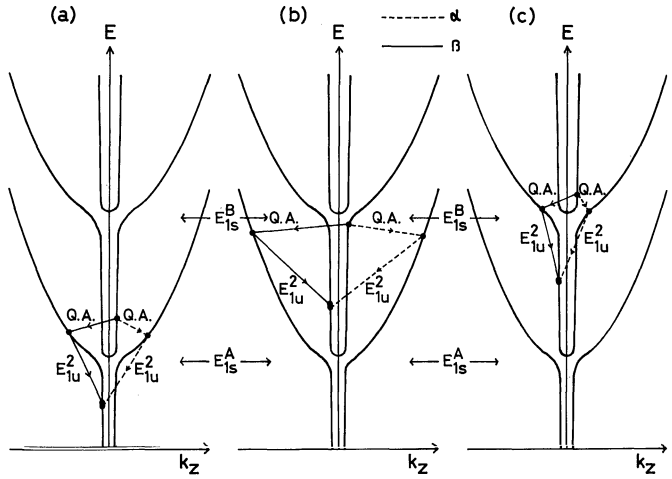


Fig. 3. Schematic Raman processes of the two-phonon scattering of polaritons by a longitudinal quasi-acoustic (Q.A.) and an $E^2_{1u}$ phonons for three different incident photon energies. (a) The incident photon energy is above the 1*s* level of the A exciton. (b) The incident photon energy is near and below the 1*s* level of the B exciton. (c) The incident photon energy is above the 1*s* level of the B exciton. The dotted lines show the $\alpha$ process, while the solid lines show the $\beta$ process.

combination of a longitudinal quasi-acoustic phonon plus an $E^1_{2g}$ phonon ($\Delta_5$) would correspond to a slightly higher frequency than the observed dispersive Raman peak and this combination along the c direction in the present experimental configuration is forbidden by group theory.

$MoS_2$ is a layered compound on the trigonal prismatic structure and the unit cell of the 2H stacking type contains two prisms of adjacent layers. Because of the weak interlayer van der Waals interaction, high-frequency optical phonons are almost dispersionless along the *c* axis and the acoustic and quasi-acoustic phonons along the *c* axis are characterized by the property that the entire atoms on a layer vibrate as a rigid unit against the neighbouring layers. The dispersion curve for the quasi-acoustic phonon can be recognized as a part of the dispersion curve for acoustic mode in a one-dimensional monatomic lattice.[19] Its frequency, therefore, is approximately described by

$$\omega_0(\boldsymbol{q}_z)=\omega_0(0)\sin(\pi/2-|\boldsymbol{q}_z|l/4), \qquad (1)$$

where $\omega_0(0)$ is the frequency at the $\Gamma$ point and $l$ the lattice constant along the *c* axis and $\boldsymbol{q}_z$ the wave vector of this phonon along the *c* axis. The longitudinal quasi-acoustic phonon is a silent mode ($B^2_{2g}$) at the $\Gamma$ point, while the transverse quasi-acoustic phonon is a Raman-active mode ($E^2_{2g}$) at the $\Gamma$ point. The former has been observed at 56 $cm^{-1}$ in neutron diffraction[18] and the latter at 33.7 $cm^{-1}$ by Verble *et al.*[19] and at 32.0 $cm^{-1}$ by Chen and Wang[20] in Raman scattering.

The dispersion of the outer branch of the polariton is nearly the same as that of exciton above the 1*s* levels of the excitons. The dispersion of the polariton can be approximately replaced by the exciton and photon dispersions. Under the assumption that the 1*s* bands of the A and B excitons are parabolic, the resonant condition is given by

$$\hbar\omega_i=E^{A,B}_{1s}+\hbar^2\boldsymbol{k}_z^2/(2M^{A,B}_{//})+\hbar\omega_0(\boldsymbol{q}_z), \qquad (2)$$

and

$$\omega_i=\pm c(|\boldsymbol{k}_z|-|\boldsymbol{q}_z|)/n_0, \qquad (3)$$

where + sign represents $\alpha$ process in Fig. 3, while − sign $\beta$ process. $E^{A,B}_{1s}$ is the energy of the 1*s* level of the A or B exciton, $\boldsymbol{k}_z$ the wave vector of the exciton along the *c* axis, $n_0$ the ordinary refractive index and *c* the velocity of light. $M^{A,B}_{//}$ is the translational mass of the A or B exciton along the *c* axis and given by

$$M^{A,B}_{//}=m^{A,B}_{e//}+m^{A,B}_{h//}, \qquad (4)$$

* Although this phonon has a large wave vector, we here call it $E^2_{1u}$, which is the representation at the $\Gamma$ point.

where $m_{e//}^{A,B}$ and $m_{h//}^{A,B}$ are effective masses of the electron and hole of the A or B exciton along the $c$ axis, respectively.

The theoretical curves are also shown in Fig. 2. We have used eqs. (1), (2) and (3) and have neglected the dispersion of the $E_{1u}^2$ phonon (its frequency is 381.0 $cm^{-1}$ from Figs. 1(a), (b) and 2). Here, using $E_{1s}^A=1.9449$ eV, $E_{1s}^B=2.1376$ eV, $l=2\times6.147$ Å (ref. 1) and $n_0=2.6$ (ref. 21), we obtain $\omega_0(0)=49$ $cm^{-1}$, $M_{//}^A=(1.3\pm0.2)m_0$ and $M_{//}^B=(1.6\pm0.3)m_0$ ($m_0$ is the mass of a free electron). The frequency difference is very small between the $\alpha$ and $\beta$ processes, which are shown by the dotted and solid curves in Fig. 2, respectively. The calculated curves are almost linear in contrast to the cases of CdS,[13] ZnTe[14] and $Cu_2O$.[15] It is due to the fact that in the vicinity of the 1$s$ levels of these excitons the wave vector of the intermediate polariton increases remarkably as $\omega_i$ increases, while the frequency of the longitudinal quasi-acoustic phonon decreases only moderately as $|\boldsymbol{q}_z|$ increases. On the other hand, far above the 1$s$ levels of these excitons the former increases only moderately as $\omega_i$ increases, while the latter decreases remarkably as $|\boldsymbol{q}_z|$ increases.

Two-phonon RRS can be used to check polariton and phonon dispersions up to a very large wave vector in comparison with the resonant Brillouin scattering. In the present experiment, we have deduced the dispersions of two phonons with $|\boldsymbol{q}_z|$ less than about 0.9 of the Brillouin-zone boundary. The theoretical curves in Fig. 2 are in good agreement with the experimental data. This result implies that the longitudinal quasi-acoustic phonon has the dispersion of eq. (1) and the 1$s$ bands of the A and B excitons are parabolic up to about 0.9 of the Brillouin-zone boundary. The resonant condition is satisfied in the region from the Brillouin-zone center to about 1/6 of the zone boundary in CdS[13] and ZnTe,[14] and to about 1/4 in $Cu_2O$.[15] The dispersions deduced from our experiments extend much farther away from the zone center than those in the multi-phonon RRS of CdS,[13] ZnTe[14] and $Cu_2O$.[15] In our two-phonon RRS the polariton-phonon interaction is governed by deformation potential. This interaction decreases rapidly if the phonon wavelength $2\pi/|\boldsymbol{q}|$ is smaller than the exciton Bohr radius.[13] In our experiment the phonon wavelength (24.6 Å) at the Brillouin-zone boundary is comparable to the Bohr radii of the A exciton (24.5 Å) and the B exciton (8.0 Å) along the $c$ axis.[22] Consequently we were able to observe the dispersions of the phonons and polaritons up to the vicinity of the zone boundary in 2H–$MoS_2$.

The frequency of the longitudinal quasi-acoustic phonon ($\omega_0(0)=49$ $cm^{-1}$) obtained by us is slightly smaller than that obtained by neutron diffraction (56 $cm^{-1}$).[18] This difference may be due to the experimental error in the neutron diffraction. In general the experimental error in Raman scattering is less than that in the neutron diffraction, in particular, in the low-frequency region.

In the layered compound 2H–$MoS_2$, the exciton bands along the $c$ axis are flatter than those in the $a$-$b$ plane and the dispersion vs $\boldsymbol{k}$ vector in the $a$-$c$ or $b$-$c$ plane forms a steep valley along the $c$ axis.[1,2,22,23] The intermediate polariton along the $c$ axis contributes to the resonant two-phonon Raman process, because of the slow group velocity[3] (see eq. (7)). Because the exciton masses have large anisotropies, the two-phonon spectrum involving phonons other than those along the $c$ axis becomes weak and broad. In this two-phonon Raman process the polariton-phonon interaction is deformation-potential type. The strength of this interaction[13] is expected to have a maximum for the wave vector parallel to the $c$ axis and falls off with increasing angle between the wave vector and the $c$ axis, but less rapidly than the piezoelectric interaction. This fact also supports the dominant contribution of the phonons along the $c$ axis. Excitons are coupled with longitudinal phonons more strongly than transverse ones. Then the longitudinal quasi-acoustic phonon predominantly contribute to this process.

On the other hand, the dominant interaction of polaritons with TA and LA phonons is piezoelectric in CdS[13] and ZnTe.[14] This piezoelectric interaction is strongly anisotropic as a function of the propagation direction of the acoustic phonons. As a result, the dispersive two-phonon Raman processes can be observed if the acoustic phonons propagate along the particular directions (for example,

[100], [110] and [111] directions in ZnTe (ref. 14)).

Oka and Cardona[14] have observed a switching from the scattering process of the acoustic-phonon emission followed by the LO-phonon emission to that of the reversed order in ZnTe. But the latter process has not been observed in CdS.[13] In 2H–$MoS_2$ we have not observed the process of the reversed order, which would be observed if $\omega_i$ becomes higher than the exciton energy plus the $E^2_{1u}$ phonon energy.

Figure 4 shows the Raman cross section $\sigma(\omega_i)$ of the dispersive Raman peak. This was obtained by correcting the Raman intensities for the absorption and reflection,[24] so that

$$\sigma(\omega_i)=\frac{(\alpha_i+\alpha_s)}{(1-R_i)(1-R_s)}I, \tag{5}$$

where $R_i$ and $R_s$ are the reflectivities at the incident and scattered wavelengths; $\alpha_i$ and $\alpha_s$ are the absorption coefficients at the incident and scattered wavelengths; $I$ is the scattered light intensity normalized by the incident laser power and the instrumental response. The Raman cross section given by the open circles does not exhibit a peak at the $1s$ level of the A exciton but at about $E^A_{1s}+\hbar\omega_b$, where $\omega_b$ is the average frequency of the dispersive Raman peak, and

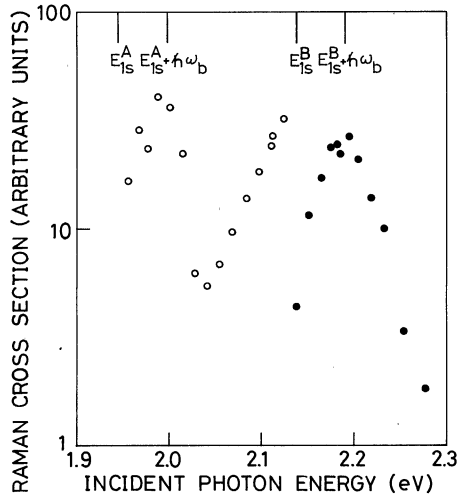


Fig. 4. Raman cross section of the dispersive Raman peak plotted as a function of the incident photon energy. Open and closed circles show Raman cross sections with the participation of the A and B excitons, respectively.

it again increases as $\omega_i$ approaches the $1s$ level of the B exciton. The Raman cross section given by the closed circles also shows a peak at $E^B_{1s}+\hbar\omega_b$. These facts indicate that the scattered light ($\omega_s$) is strongly resonant with the $1s$ levels of the A and B excitons.

The Raman cross section of the second-order Raman process shown in Fig. 3 can be written in polariton picture[6,25,26] as follows

$$\sigma(\omega_i)\propto\frac{1}{v_g^i}\sum_{q_1q_2}\left|\frac{\langle k_i|V|k\rangle\langle k|V|k_s\rangle}{\omega_{pol}(k_i)-\omega_{pol}(k)-\omega_0(q_1)-i\gamma}\right|^2 \times\delta(\omega_{pol}(k_i)-\omega_{pol}(k_s)-\omega_0(q_1)-\omega_0'(q_2))\delta(k_i-k_s-q_1-q_2), \tag{6}$$

where $v_g^i$ is the group velocity of the initial polariton, $k_i$, $k$ $(=k_i-q_1)$ and $k_s$ are the wave vectors of the initial, intermediate and final polaritons, respectively. $V$ is the polariton-phonon interaction Hamiltonian, $\omega_{pol}(k)$ is the frequency of the polariton, $\gamma$ is the damping constant of the intermediate polariton, and $\omega_0'(q)$ is the frequency of the $E^2_{1u}$ phonon which is independent of $q$. Under the assumption that only the phonons and polaritons along the $c$ axis participate in this RRS and that $\gamma$ is small, i.e., the resonant condition is satisfied, we obtain

$$\sigma(\omega_i)\propto\frac{1}{v_g^i(v_g'+v_g^0)(v_g^s+v_g^{0\prime})}\frac{\pi}{\gamma}|\langle k_i|V|k_z\rangle\langle k_z|V|k_s\rangle|^2 \approx\frac{1}{v_g^iv_g'v_g^s}\frac{\pi}{\gamma}|\langle k_i|V|k_z\rangle\langle k_z|V|k_s\rangle|^2, \tag{7}$$

where $v_g'$ and $v_g^s$ are the group velocities of the intermediate and final polaritons, respectively; $v_g^{0\prime}$ is the group velocity of the longitudinal quasi-acoustic phonon and much smaller than $v_g'$; $v_g^{0\prime}$ is the group velocity of the $E^2_{1u}$ phonon and equal to zero by assumption. Here the dispersion of the intermediate polariton is approximated by the exciton dispersion and we can use eq. (2) as a resonant condition. The variation of $\gamma$ is small and that of $\langle k_i|V|k_z\rangle$

$\times \langle \boldsymbol{k}_z|V|\boldsymbol{k}_s\rangle$ is also small except when the intermediate polariton with a small $\boldsymbol{k}_z$ participates in this Raman process, because the two-phonon process consisting of the longitudinal quasi-acoustic phonon and the $E^2_{1u}$ phonon along the $c$ axis is allowed except for the $\Gamma$ point by group theory. Then the strong enhancement is associated with the smallness of the group velocities if the energies of the incident and scattered light approach the exciton levels. If the incident polariton lies near the bottom of the inner branch, $v_g^i$ is very small. The phonons with small $\boldsymbol{q}_z$ participate in this case. Then the matrix element $\langle \boldsymbol{k}_i|V|\boldsymbol{k}_z\rangle\langle \boldsymbol{k}_z|V|\boldsymbol{k}_s\rangle$ is expected to be small and the Raman cross section is small. Far above the bottom of the inner polariton branch, as shown in Fig. 3(a), the two-phonon process with large $\boldsymbol{q}_z$ is Raman active and we can set $v_g^i \cong c/n_0$. Because the frequency of the longitudinal quasi-acoustic phonon $\omega_0(\boldsymbol{q}_z)$ is small, $v_g'$ is approximately proportional to $|\boldsymbol{k}_z|$ and therefore it varies gradually in the case shown in Fig. 3(a). This fact has been pointed out by Bendow and Birman (see Fig. 2 of ref. 26). If the energy of the scattered light approaches the $1s$ level of the A exciton from below, $v_g^s$ becomes remarkably small and has a minimum at $\hbar\omega_s \cong E^A_{1s}$. As a result, the Raman cross section exhibits a peak at $\hbar\omega_s \cong E^A_{1s}$ and not at $\hbar\omega_i \cong E^A_{1s}$. Moreover for $\hbar\omega_i \to E^B_{1s}$, as shown in Fig. 3(b), $v_g^i$ becomes small and therefore the Raman cross section is again enhanced. If $\omega_i$ is immediately above the bottom of the inner branch of the B exciton-polariton, as shown in Fig. 3(c), the same circumstance occurs as in the case of the A exciton, and then the Raman cross section weakens distinguishedly. For $\hbar\omega_s \cong E^B_{1s}$, the Raman cross section has a maximum again. The qualitative explanation described above is in good agreement with the Raman cross section of the dispersive Raman peak observed in Fig. 4. This fact verifies that the dispersive Raman peak comes from the Raman processes shown in Fig. 3.

Dispersive two-phonon modes of CdS[13] and ZnTe[14] can be observed if $\hbar\omega_i$ is just above the lowest energy of the inner polariton branch, and not if $\hbar\omega_i = E_{1s}$. Because the energy difference between the lowest energy of the inner polariton branch and $E_{1s}$ has not been observed clearly in the present experiment, the frequency shift of the dispersive Raman mode in 2H–$MoS_2$ can be also explained by the exciton model. Moreover this model can explain the Raman cross section. It also leads to the same conclusion that the dispersive Raman mode can be identified as a two-phonon Raman spectrum with the successive emission of the longitudinal quasi-acoustic phonon and the $E^2_{1u}$ phonon both along the $c$ axis.

## §4. Conclusion

We have observed a dispersive Raman peak in 2H–$MoS_2$ for the case where $\omega_i$ is above the $1s$ levels of the A and B excitons. The frequency shift decreases as $\omega_i$ goes away from the $1s$ states of the A and B excitons and this feature is contrary to those observed in CdS,[13] ZnTe[14] and $Cu_2O$.[15] This result can be interpreted in terms of a two-phonon Raman process of the successive emission of a dispersive longitudinal quasi-acoustic phonon and a dispersionless $E^2_{1u}$ phonon both along the $c$ direction. Under the assumption that the dispersion of the longitudinal quasi-acoustic phonon along the $c$ axis is written as eq. (1), the translational exciton masses along the $c$ axis have been estimated to be $(1.3\pm0.2)m_0$ for the $1s$ state of the A exciton and $(1.6\pm0.3)m_0$ for the $1s$ state of the B exciton. In the present experiment we have deduced two phonons with their $|\boldsymbol{q}_z|$ up to about 0.9 of the Brillouin-zone boundary contributing to the dispersive second-order Raman peak. The success in the observation of the dispersive second-order Raman peak consisting of two optical phonons is mainly due to the fact that the dispersions of polaritons (or excitons) along the $c$ axis are much flatter than those in the $a$-$b$ plane. This property comes from the two-dimensional character of the layered structure in 2H–$MoS_2$. What mentioned above contrasts the fact that the dispersive Raman peaks already observed in CdS and ZnTe are due to the anisotropic piezoelectric interaction of polariton with the TA and LA phonons. The relative magnitude of the Raman cross section for this peak is consistent with qualitative estimation in terms of this Raman process.

## Acknowledgement

The authors would like to thank Dr. M. Izumi for helpful assistance in the experiment and for stimulating discussion.

## References

1) J. A. Wilson and A. D. Yoffe: Adv. Phys. **18** (1969) 193.
2) B. I. Evans: *Optical and Electrical Properties* (*Physics and Chemistry of Materials with Layered Structures*, Vol. 4), ed. P. A. Lee (Reidel, Dordrecht, 1976) p. 1.
3) R. G. Ulbrich and C. Weisbuch: Phys. Rev. Lett. **38** (1977) 865.
4) R. Sooryakumar and P. E. Simonds: Solid State Commun. **42** (1982) 287.
5) G. Winterling and E. S. Koteles: Solid State Commun. **23** (1977) 95; G. Winterling, E. S. Koteles and M. Cardona: Phys. Rev. Lett. **39** (1977) 1286; E. S. Koteles and G. Winterling: Phys. Rev. Lett. **44** (1980) 948.
6) P. Y. Yu and F. Evangelisti: Solid State Commun. **27** (1978) 87.
7) R. G. Ulblich and C. Weisbuch: *Festkürperprobleme* (Advances in Solid State Physics) Vol. XVIII, ed. J. Treusch (Vieweg, Braunschweig, 1978) p. 217.
8) C. Hermann and P. Y. Yu: Solid State Commun. **28** (1978) 313; Phys. Rev. **B21** (1980) 3675.
9) B. Sermage and G. Fishman: Phys. Rev. Lett. **43** (1979) 1043.
10) T. Goto and Y. Nishina: Solid State Commun. **31** (1979) 751.
11) T. Goto: J. Phys. Soc. Jpn. **51** (1982) 3.
12) D. P. Vu, Y. Oka and M. Cardona: Phys. Rev. **B24** (1981) 765.
13) E. S. Koteles and G. Winterling: Phys. Rev. **B20** (1979) 628.
14) Y. Oka and M. Cardona: Solid State Commun. **30** (1979) 447.
15) P. Y. Yu and Y. R. Shen: Phys. Rev. Lett. **32** (1974) 939; Phys. Rev. **B12** (1975) 1377.
16) T. Sekine, T. Nakashizu, M. Izumi, K. Toyoda, K. Uchinokura and E. Matsuura: *Proc. 15th Int. Conf. Physics Semiconductors, Kyoto, 1980*, J. Phys. Soc. Jpn. **49** (1980) Suppl. A, p. 551.
17) T. Sekine, M. Izumi, T. Nakashizu, K. Uchinokura and E. Matsuura: J. Phys. Soc. Jpn. **49** (1980) 1069.
18) N. Wakabayashi, H. G. Smith and R. M. Nicklow: Bull. Am. Phys. Soc. II **17** (1972) 292; Phys. Rev. **B12** (1975) 659.
19) J. L. Verble, T. J. Wieting and P. R. Reed: Solid State Commun. **11** (1972) 941.
20) J. M. Chen and C. S. Wang: Solid State Commun. **14** (1974) 857.
21) B. L. Evans and P. A. Young: Proc. R. Soc. London **A284** (1965) 402.
22) B. L. Evans and P. A. Young: Phys. Status Solidi **25** (1968) 417.
23) B. L. Evans and P. A. Young: Proc. Phys. Soc. **91** (1967) 475; R. A. Bromley, R. B. Murray and A. D. Yoffe: J. Phys. **C5** (1972) 759; R. V. Kasowski: Phys. Rev. Lett. **30** (1973) 1175; R. A. Neville and B. L. Evans: Phys. Status. Solidi (b) **73** (1976) 597.
24) R. Loudon: J. Phys. (France) **26** (1965) 677.
25) B. Bendow: *Electrical Structure of Noble Metals and Polariton-Mediated Light Scattering* (*Springer Tracts in Modern Physics*, Vol. 82), (Springer-Verlag, Berlin, 1978) p. 69.
26) B. Bendow and J. L. Birman: Phys. Rev. **B1** (1970) 1678.